

# A K-Band Ground-Backed CPW Balanced Coupler and Integrated Antenna Feed

Michael Forman and Zoya Popović

University of Colorado  
Boulder, CO 80309-0425 USA  
[Michael.Forman@Colorado.EDU](mailto:Michael.Forman@Colorado.EDU)

**Abstract**—This paper reports on the performance of a *K*-band finite-width ground-backed CPW balanced coupler. The use of the coupler as a balanced feed for a slot and patch antenna is investigated. The designs are uniplanar and the circuit does not require vias or airbridges. The return loss of the coupler is less than 10 dB over a 12% bandwidth from 17.1 to 19.2 GHz with a 2-dB average insertion loss over the pass band. The 2:1-VSWR bandwidths of the transition-fed slot and patch antenna are 3.3% and 3.1% respectively.

## I. INTRODUCTION

Coplanar waveguide (CPW) is utilized in many commercial microwave circuits where uniplanar fabrication is required. CPW conveniently provides a signal line and ground plane on the same side of the substrate, which eliminates the need for vias commonly used with microstrip transmission lines (MSL). To reduce cost and complexity in multilayer integrated circuits where RF connectivity between layers is required, it is desirable to keep fabrication limited to uniplanar processing, thus ruling out other interconnects such as vias or embedded coax.

Due to mechanical and thermal requirements, the substrates for coplanar monolithic microwave integrated circuits (CMMIC) are metalized on one side. The resulting transmission line is referred to as conductor-backed CPW (CBCPW) [1]. In practice the two CPW ground electrodes are limited in width in order to suppress leaky parallel-plate modes. These unwanted modes would otherwise be supported between the side grounds and the substrate ground. This type of transmission line is known as finite-width ground-backed coplanar waveguide (FW-GBCPW) [1], referred to as fCPW in this paper for brevity.

Uniplanar circuit elements recently developed for CMMICs on either finite-ground CPW (FGCPW) or fCPW are filters [2], lumped elements [3] and mul-

This work is supported by Caltech through the Army Research Organization Multidisciplinary Research Initiative Program on “Quasi-Optical Power Combining” under contract DAAH04-98-0-0001.

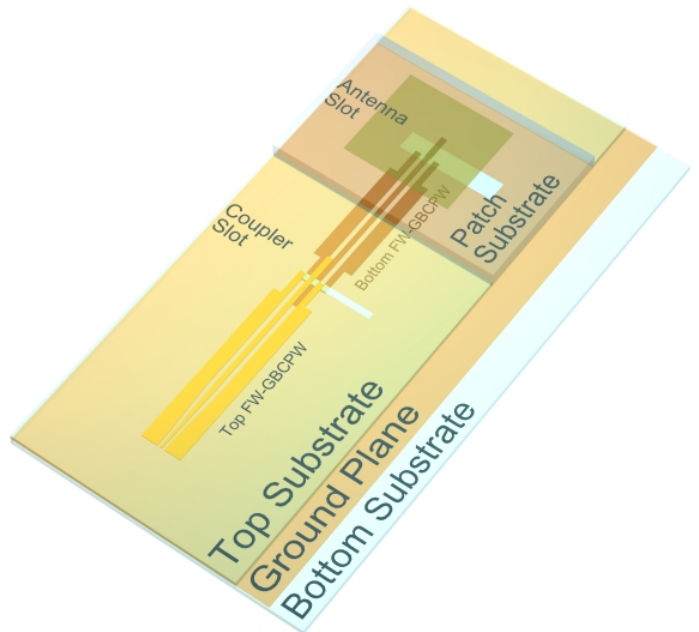


Fig. 1. Perspective rendering of the *K*-band ground-backed CPW balanced coupler with the transition-fed patch antenna. The circuits are uniplanar in design and do not require vias or airbridges. Signals are coupled electromagnetically through the slots in the shared ground plane.

tipliers [4]. The balanced fCPW-to-fCPW transition presented in this paper is an extension to the recently developed fCPW-to-MSL [5] and FGCPW-to-FGCPW transitions [6].

## II. DESIGN

The substrate used for the transmission lines and slots is Rogers TMM10i which has a thickness of  $381\ \mu\text{m}$ , a relative permittivity of  $\epsilon_r = 9.806$ , a loss tangent of  $\tan\delta = 0.002$ , and a metal thickness of  $17.5\ \mu\text{m}$ . To prevent loss due to surface waves, the substrate was chosen to be thin ( $\lambda_d/13$ ) relative to the dielectric wavelength [7].

The dimensions of the  $50\text{-}\Omega$  fCPW are constrained by:

- Matching the inner fCPW conductor width ( $w_{\text{cpw}}$ ) to the MSL width ( $w_{\text{ms}}$ ). The limit being  $(2s_{\text{cpw}} +$

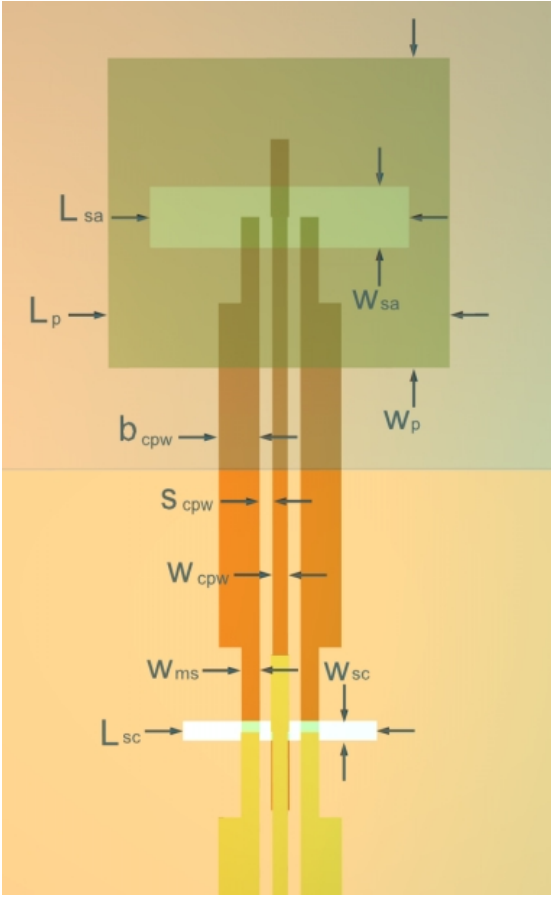


Fig. 2. Balanced coupler and patch antenna with dimensions labeled.

$$w_{cpw} \geq w_{ms}.$$

- Setting the ratio of the width fCPW to the substrate height  $((2s_{cpw} + w_{cpw})/h)$  to a value which provides sufficient coupling to the shared ground plane without exciting the unwanted higher-order MSL mode [8].
- Choosing practical widths ( $w_{cpw}$ ) and gaps ( $s_{cpw}$ ) which can be fabricated and measured accurately and repeatably.

The design of the coupler and antennas is performed by starting from zero-order physical-reasoning and optimizing the design using the commercial full-wave simulation tool *IE3D* [9] (Fig. 3).

The slot coupler is comprised of two fCPW-to-MSL transitions aligned on opposite sides of a slot in a shared substrate ground plane (Fig. 1). The transition from fCPW to MSL occurs in three coupled microstrip transmission lines. The transition lengths are  $\lambda_{ms}/4$  at the center frequency of operation ( $f_0 = 19$  GHz), where  $\lambda_{ms}$  is the guided wavelength of the three-conductor (MSL) lines [5]. The slot in the substrate ground is centered between the interface of the three  $\lambda_{ms}/4$  coupled MSL sections and the single  $\lambda_{ms}/4$  MSL (Fig. 2).

For the antennas, one side of the coupler is used as

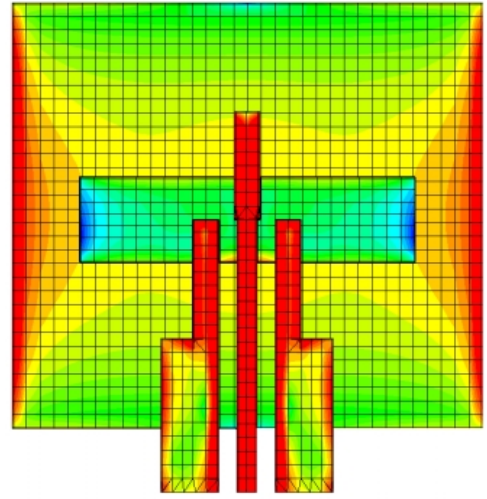


Fig. 3. Simulated average current density on the slot-fed patch antenna.

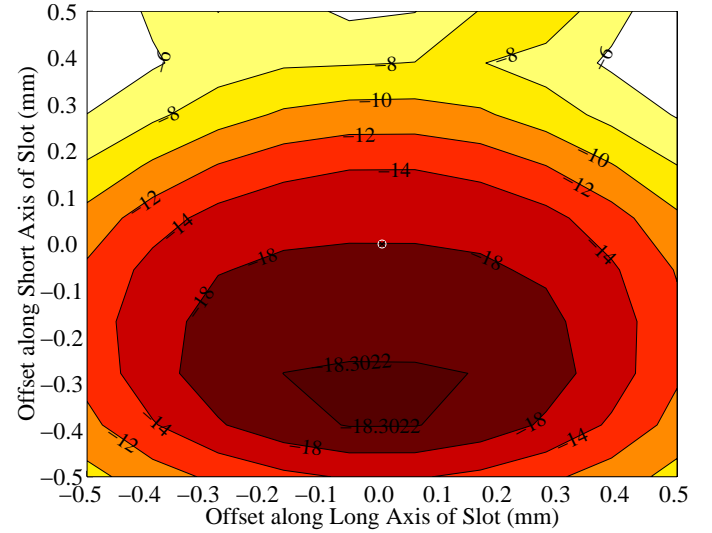


Fig. 4. Sensitivity analysis with respect to transition-to-slot misalignment along both axes. The contour plots show values of  $S_{11}$  in dB at 19 GHz.

the feed and the slot is optimized for radiation instead of coupling. This method differs from the one presented in [10], in that the transition is combined with the radiating slot to reduce real estate requirements.

To avoid the low radiation efficiency typical of microstrip antennas fabricated on thin, high-permittivity substrates, the patch antenna is placed on a low-permittivity dielectric above the slot. The dielectric is Rohacell 31 HF with a thickness of 1 mm, a relative permittivity of  $\epsilon_r = 1.07$ , and a loss tangent of  $\tan \delta = 0.0036$  at the design frequency. The dimensions of the transmission lines, slot couplers, and substrates are summarized in Table 2.

Table 1: TRANSMISSION LINE SPECIFICATIONS

fCPW Dimensions		Microstrip Dimensions		Substrate Values	
$w_{\text{cpw}}$	300 $\mu\text{m}$	$w_{\text{ms}}$	360 $\mu\text{m}$	$\epsilon_r$	9.806
$s_{\text{cpw}}$	250 $\mu\text{m}$	$\lambda_{\text{ms}}$	6.1 mm	$\tan \delta$	0.002
$b_{\text{cpw}}$	800 $\mu\text{m}$			$h$	381 $\mu\text{m}$
$\lambda_{\text{cpw}}$	6.7 mm			$t$	17.5 $\mu\text{m}$

Table 2: COUPLER AND ANTENNA DIMENSIONS

Coupler Dimensions		Slot Dimensions		Patch Dimensions	
$l_{\text{sc}}$	3.57 mm	$l_{\text{sa}}$	4.67 mm	$l_{\text{p}}$	6.56 mm
$w_{\text{sc}}$	0.38 mm	$w_{\text{sa}}$	1.20 mm	$w_{\text{p}}$	5.99 mm
				$h_{\text{p}}$	1.00 mm

### III. FABRICATION

The fabrication and alignment of the circuits are performed in alternate steps of milling and photolithography. The steps in the fabrication process are: milling substrate “blanks” with alignment holes suitable in size for photolithography; processing the front and back of the substrate with standard photolithography; and assembling the individual components by means of milling, stacking, and aligning into a multilayer circuit.

In order to achieve the alignment requirements while using an inexpensive technique, a single alignment jig capable of holding the substrate through all steps of fabrication is used. The jig consists of an aluminum plate with pins on the top for substrate alignment and pins on the bottom for repeatable mating to the working surface of a milling machine. A removable glass plate attaches to the jig during the photolithography exposure step to pressure-fit the mask to the substrate.

This process achieves accuracies of  $\pm 50 \mu\text{m}$  in mask-to-substrate alignment and  $\pm 50 \mu\text{m}$  for substrate-to-substrate (multilayer) alignment. In order to predict the effect of alignment variation, a sensitivity analysis was performed and the results are shown in Fig. 4. The slot can be misaligned by  $\pm 500 \mu\text{m}$  ( $\pm 0.075\lambda_{\text{cpw}}$ ) relative to the feed and still maintain a -10 dB return loss. Perturbation simulations for the antennas show similar trends.

### IV. MEASUREMENTS

The S-parameters of the slot-coupler transition are measured using an HP 8510 network analyzer. The VNA is calibrated with a TRL calibration fabricated on the same substrate as the DUT. The measured performance of the transition is compared with the *IE3D* Method-of-Moment simulation in Fig. 6 and Fig. 7.

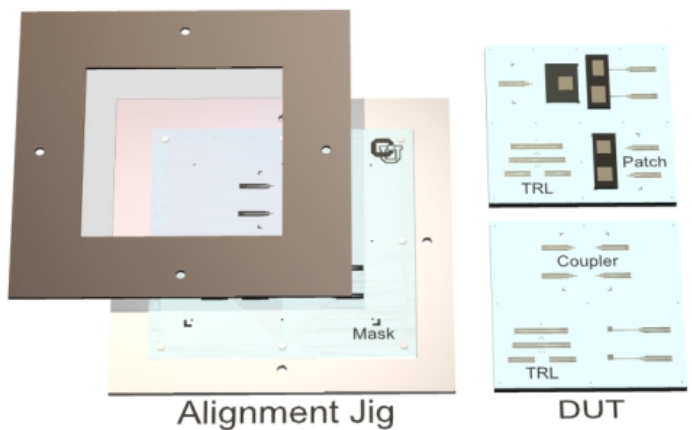


Fig. 5. The alignment jig is shown on the left with a substrate “blank” and mask on the alignment pins. The assembled multilayer circuits are shown on the right with the coupler, patch antenna, and TRL calibration set labeled.

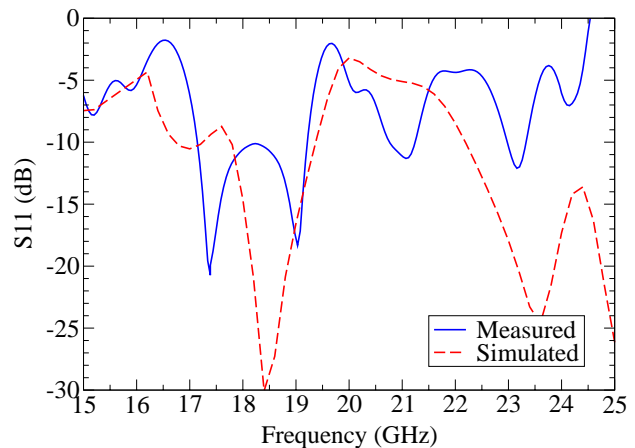


Fig. 6. Measured and simulated reflection coefficient of the slot coupler.

The measured return loss of the coupler is less than 10 dB over a 12% bandwidth from 17.1 to 19.2 GHz with a 2 dB average insertion loss over the pass band. Because the DUT is measured with probes, two slot couplers are connected and measured in series. The measured coupler is shown and labeled in Fig. 5.

The performance of the transition-fed slot and patch antennas is shown in Fig. 8 and Fig. 9 respectively. The slot antenna’s measured center frequency is 18.35 GHz, a deviation of -3.4% from the simulated resonance. The measured bandwidth of the slot antenna is 3.3% with a simulated efficiency of 63% and a directivity of 5.4 dB. The slot radiates preferentially in the direction of the substrate with a front-to-back ratio of 5 dB. The shift in resonance is attributed to widening of the slot due to overetching during fabrication.

The measured bandwidth of the patch antenna is

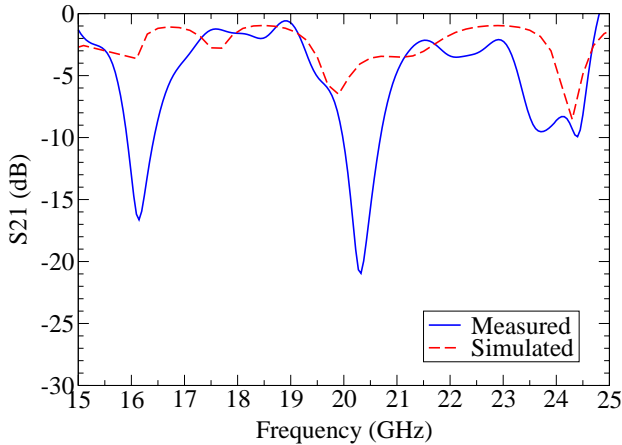


Fig. 7. Measured and simulated transmission coefficient of the slot coupler.

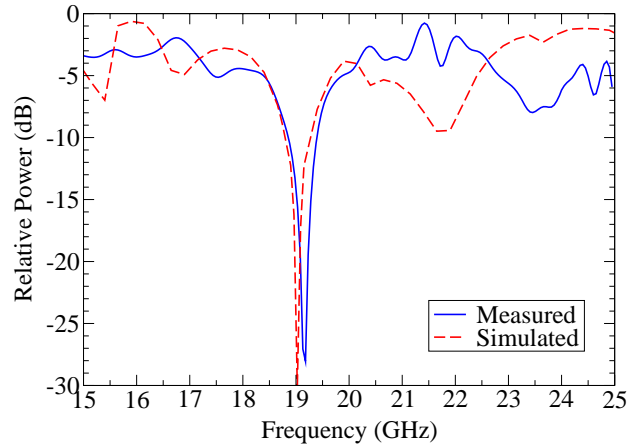


Fig. 9. Measured and simulated reflection coefficient of the slot-fed patch antenna.

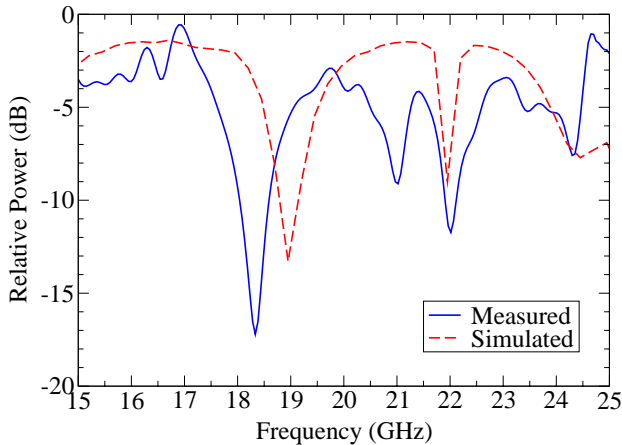


Fig. 8. Measured and simulated reflection coefficient of the slot antenna.

3.1% with a simulated efficiency of 80% and directivity of 9.2 dB. The front-to-back ratio is 20 dB. Because the patch antenna was milled and attached after the photolithography step, there is no overetch error and the measured and simulated center frequencies agree within 1%.

The coupler and antenna feed presented in this paper were developed as elements in an active amplifier array. The active array operates in full-duplex transmit-receive mode and requires an up- and down-link frequency. The coupler-feed design accommodates easy frequency scaling, allowing quick prototyping and trade-off analysis.

## REFERENCES

[1] Y. C. Shih and T. Itoh, "Analysis of conductor-backed coplanar waveguide," *Electron. Lett.*, vol. 18, pp. 538–540,

June 1982.  
 [2] K. J. Herrick, T. Schwarz, and L. P. B. Katehi, "W-band micromachined finite ground coplanar (FGC) line circuit elements," *IEEE Trans. Microwave Theory Tech.*, vol. 1, pp. 269, 1997.  
 [3] Fred Brauchler, Steve Robertson, Jack East, and Linda P. B. Katehi, "W-band finite ground coplanar (FGC) line circuit elements," *IEEE Trans. Microwave Theory Tech.*, vol. 3, 1996.  
 [4] J. Papapolymerou, F. Brauchler, J. East, and L. P. B. Katehi, "W-band finite ground coplanar monolithic multipliers," *IEEE Trans. Microwave Theory Tech.*, vol. 75, no. 5, pp. 614, 1999.  
 [5] Gildas P. Gauthier, Linda P. Katehi, and Gabriel M. Rebeiz, "W-band finite ground coplanar waveguide (FGCPW) to microstrip line transition," *IEEE Trans. Microwave Theory Tech.*, vol. 1, pp. 107, 1998.  
 [6] Jean-Pierre Raskin, Gildas Gauthier, Linda P. Katehi, and Gabriel M. Rebeiz, "W-band single-layer vertical transitions," *IEEE Trans. Microwave Theory Tech.*, vol. 48, no. 1, pp. 161–164, 2000.  
 [7] A. Vandelay, M. Von Nostrand, and K. Varnsen, "Signed-field analysis of surface mode losses," *IEEE Microwave and Guided Wave Lett.*, 1989.  
 [8] Ching-Cheng Tien, Ching-Kuang C. Tzuang, S. T. Peng, and Chung-Chi Chang, "Transmission characteristics of finite-width conductor-backed coplanar waveguide," *IEEE Trans. Microwave Theory Tech.*, pp. 1616–1623, Sept. 1993.  
 [9] IE3D Version 7.01, Zeland Software Inc., 39120 Argonaut WY STE 499, Fremont, CA 94538 USA.  
 [10] Gildas P. Gauthier, Jean-Pierre Raskin, Linda P. B. Katehi, and Gabriel M. Rebeiz, "A 94-ghz aperature-coupled micromachined microstrip antenna," *IEEE Trans. Ant. and Prop.*, vol. 47, no. 12, Dec. 1999.